

## EMBRITTLMENT OF Cr-Mo STEELS AFTER LOW FLUENCE IRRADIATION IN HFIR – R. L. Klueh and D. J. Alexander

### OBJECTIVE

The goal of this work is the determination of the possible effect of the simultaneous formation of helium and displacement damage during irradiation on the Charpy impact behavior.

### SUMMARY

Subsize Charpy impact specimens of 9Cr-1MoVNb (modified 9Cr-1Mo) and 12Cr-1MoVW (Sandvik HT9) steels and 12Cr-1MoVW with 2% Ni (12Cr-1MoVW-2Ni) were irradiated in the High Flux Isotope Reactor (HFIR) at 300 and 400°C to damage levels up to 2.5 dpa. The objective was to study the effect of the simultaneous formation of displacement damage and transmutation helium on impact toughness. Displacement damage was produced by fast neutrons, and helium was formed by the reaction of  $^{58}\text{Ni}$  with thermal neutrons in the mixed-neutron spectrum of HFIR. Despite the low fluence relative to previous irradiations of these steels, significant increases in the ductile-brittle transition temperature (DBTT) occurred. The 12Cr-1MoVW-2Ni steel irradiated at 400°C had the largest increase in DBTT and displayed indications of intergranular fracture. A mechanism is proposed to explain how helium can affect the fracture behavior of this latter steel in the present tests, and how it affected all three steels in previous experiments, where the steels were irradiated to higher fluences.

### PROGRESS AND STATUS

#### Introduction

In addition to the displacement damage formed in a fusion power plant first wall by high-energy neutrons from the fusion reaction, helium will be formed by transmutation. About 110 appm He will form in a martensitic steel in one year of operation at a wall loading of 1 MW/m<sup>2</sup>. This contrasts with <6 appm He formed in the steel irradiated for one year in a fast reactor, even though the displacement damage is similar. Irradiation of ferritic steels in a fast reactor below  $\approx 450^\circ\text{C}$  can cause an increase in strength. This increase in strength is accompanied by an increase in the ductile-brittle transition temperature (DBTT), and a decrease in the upper-shelf energy (USE), as measured in a Charpy test [1-7]. DBTT values can be raised to well above room temperature.

Because no operating fusion reactors are available, simulation techniques are used to study the simultaneous effects of displacement damage and transmutation helium. One simulation technique involves adding nickel to the ferritic/martensitic steels and irradiating them in a mixed-spectrum reactor, such as the High Flux Isotope Reactor (HFIR) [8]. Displacement damage is produced by the fast neutrons in the spectrum, and helium is generated from  $^{58}\text{Ni}$  by a two-step transmutation reaction with the thermal neutrons in the spectrum. For a ferritic steel containing 2% Ni, the He/dpa ratio produced during irradiation in HFIR approximates that of a tokamak reactor. This technique has been used to examine the effect of helium on swelling at 300 to 600°C [9-11], on tensile properties after irradiation at 50, 300, 400, and 500°C [12-14], and on impact properties of subsized Charpy specimens irradiated at 50, 300, and 400°C [3,7,15].

Data have been published for the 9Cr-1MoVNb (modified 9Cr-1Mo) and 12Cr-1MoVW (the Sandvik HT9 composition) steels and these steels with up to 2% Ni irradiated to  $\approx 27$  and 40 dpa at 300 and 400°C, respectively, in the HFIR [15]. The shifts in DBTT observed after irradiation at 400°C were the largest ever observed for these steels. Steels with 2% Ni showed a larger effect than steels without the nickel additions. Furthermore, the steels that contained helium developed much larger shifts than those irradiated in a fast reactor, where little helium formed during irradiation.

For this paper, Charpy impact specimens of 9Cr-1MoVNb and 12Cr-1MoVW steels and the 12Cr-1MoVW steel with 2% Ni (12Cr-1MoVW-2Ni) were irradiated in the HFIR at 300 and 400°C to 2.5 dpa or less. The results were compared with results from doped and undoped steels irradiated to higher fluences in the HFIR [3,15] and in fast reactors [2,4,6]. Note that fluences of 2.5 dpa and less are designated "low" fluences in this paper. By low, it is meant that they are low relative to previous HFIR and fast reactor experiments, to which they will be compared. It is recognized that even these "low" fluences are high (by several orders of magnitude) relative to fluences under which some pressure vessel steels are embrittled when irradiated in a light water reactor.

#### Experimental Procedure

The 9Cr-1MoVNb (heat XA 3590), 12Cr-1MoVW (heat XAA 3587), and 12Cr-1MoVW-2Ni (heat XAA 3589) steels were 25-kg electroslag-remelted (ESR) heats prepared by Combustion Engineering, Inc., Chattanooga, Tennessee. These heats were irradiated previously in the HFIR [3,7,12-15] and the EBR-II [4]. Chemical compositions are given in Table 1.

Table 1. Composition of 9Cr-1MoVNb and 12Cr-1MoVW Heats of Steel

Element	Concentration (wt%)		
	9Cr-1MoVNb (XA 3590)	12Cr-1MoVW (XAA 3587)	12Cr-1MoVW-2Ni (XAA 3589)
C	0.09	0.21	0.20
Mn	0.36	0.50	0.49
P	0.008	0.011	0.011
S	0.004	0.004	0.004
Si	0.08	0.18	0.14
Ni	0.11	0.43	2.27
Cr	8.62	11.99	11.71
Mo	0.98	0.93	1.02
V	0.21	0.27	0.31
Nb	0.063	0.018	0.015
Ti	0.002	0.003	0.003
Co	0.013	0.017	0.021
Cu	0.03	0.05	0.05
Al	0.013	0.030	0.028
B	<0.001	<0.001	<0.001
W	0.01	0.54	0.54
As	<0.001	<0.001	<0.001
Sn	0.003	0.002	0.002
Zr	<0.001	<0.001	<0.001
N	0.050	0.020	0.017
O	0.007	0.005	0.007
Fe	Bal	Bal	Bal

Charpy impact specimens were machined from 63.5-mm-thick hot-rolled plate in the normalized-and-tempered condition. The austenitizing treatment for the 9Cr-1MoVNb steel was 0.5 h at 1040°C and for the 12Cr-1MoVW and 12Cr-1MoVW-2Ni steels was 0.5 h at 1050°C, after which they were air cooled. Tempering was for 1 h at 760°C for 9Cr-1MoVNb, for 2.5 h at 780°C for 12Cr-1MoVW, and for 5 h at 700°C for 12Cr-1MoVW-2Ni. Tempered martensite microstructures were obtained by such heat treatments. Details on heat treatment and microstructure have been published [8].

Miniature Charpy specimens were machined from the heat-treated plate in the longitudinal (L-T) orientation. The subsize specimens were one-half the standard size: 5 by 5 by 25.4 mm with a 0.76-mm-deep 30° V-notch with a 0.05- to 0.08-mm-root radius. Such miniature specimens show a transition from

ductile to brittle fracture similar to that found in full-sized Charpy specimens, although over a different temperature range [16,17].

Two capsules, each containing 16 specimens of the three steels, were irradiated in the HFIR at nominal temperatures of 300 and 400°C. For irradiation, specimens were enclosed in stainless steel holders, and the holders were placed inside aluminum sleeves. Nuclear heating was used to achieve the desired temperature. To control the temperature, the gas gap between the outer diameter of the steel specimen holder and the aluminum sleeve was adjusted to compensate for the variation in nuclear heating rate along the length of the capsule. (Instrumented capsules have been used previously to verify nuclear heating rates.) A thermal gradient exists from the interior to the exterior surface of the specimens; this has been calculated to be less than 45°C. Three flux monitors were loaded into each capsule, and they were analyzed to determine the fluences achieved. Displacement damage and helium concentrations were calculated based on these fluences.

The specimens were intended to be irradiated to 10 dpa. Unfortunately, they were inserted into the HFIR just prior to the unforeseen suspension of operation of the reactor. Because of the reduction in operating power from 100 to 85 MW when HFIR was restarted, it was decided not to irradiate the specimens beyond the one 22-day cycle they obtained when originally inserted.

The capsules were irradiated in a peripheral target position of the HFIR to a maximum total fluence of  $\approx 8.4 \times 10^{25} \text{n/m}^2$ , a maximum fast fluence of  $\approx 2.3 \times 10^{25} \text{n/m}^2$  ( $E > 0.11 \text{ MeV}$ ), and a thermal fluence of  $\approx 3.4 \times 10^{25} \text{n/m}^2$ . At the capsule midplane, a displacement-damage level of  $\approx 2.5 \text{ dpa}$  was obtained. The fluence decreased symmetrically with distance from the midplane, and the displacement-damage levels at the ends of the capsules were  $\approx 1.1 \text{ dpa}$ . Displacement-damage levels for specimens between the midplane and the ends varied systematically between these limits. Similarly, helium levels varied, depending on the position of the specimens in the capsule and the amount of nickel in the alloys. Specimens irradiated at 300°C were near the ends of the capsules, which meant they were irradiated to the lowest dpa and contained the least helium. Because of space limitations, a limited number of specimens were irradiated (six each for the 9Cr-1MoVNb and 12Cr-1MoVW steels, but only four specimens for the 12Cr-1MoVW-2Ni steel).

Charpy tests were conducted in a pendulum-type, instrumented impact machine modified for subsize specimens [17,18]. To obtain the DBTT and USE, impact energy-temperature curves were generated by fitting the data with a hyperbolic tangent function. The primary objective was the determination of the shift in DBTT. The DBTT was determined for the energy corresponding to half of the USE and at fixed energy levels of 5.5 and 9.2 J (analogous to the 41 and 68 J often used for full-size Charpy specimens) [17].

## Results

Table 2 shows the results for the Charpy impact tests. The DBTT and USE are given, along with the shift in DBTT ( $\Delta \text{DBTT}$ ) calculated using the DBTT determined at one-half the USE. Displacement-damage levels and helium concentrations for each set of specimens are given. Specimens irradiated at 400°C had damage levels of 2.1 to 2.5 dpa, and those irradiated at 300°C were 1.1 to 2 dpa.

Helium concentrations were small and varied, depending on the nickel concentration of the steel and the fluence achieved. Because the 9Cr-1MoVNb steel contained only 0.1% Ni, compared to 0.4% in the 12Cr-1MoVW steel (Table 1), it contained  $< 1 \text{ appm He}$  at both 300 and 400°C. The maximum helium concentration in the 12Cr-1MoVW steel was slightly more than 1 appm. The most helium was  $\approx 3.5 \text{ appm}$  in the 12Cr-1MoVW-2Ni irradiated at 400°C. At 300°C, this steel contained less than half this amount, because the specimens were at the ends of the capsule, where they received 1.5 dpa or less.

Despite the low fluences, large shifts in DBTT occurred. The steels without a nickel addition--the 9Cr-1MoVNb and 12Cr-1MoVW steels--developed a larger  $\Delta \text{DBTT}$  at 300°C than at 400°C. For 12Cr-1MoVW-2Ni steel, however, the  $\Delta \text{DBTT}$  at 400°C was larger than at 300°C.

Table 2. Impact Properties of Cr-Mo Steels Irradiated in HFIR

Conditions			Transition Temperature (°C)			$\Delta$ DBTT <sup>a</sup>	Use
Temp. (°C)	Displ. (dpa)	He (appm)	5.5J	9.2J	1/2 USE	(°C)	(J)
<u>12Cr-1MoVW (Heat XAA 3587)</u>							
Control	0	0	-58	-35	-18	26	
300	1.1-2.0	0.4-1.0	150	123	148	166	17
400	2.2-2.5	1.0-1.3	106	141	128	146	16
<u>12-Cr-1MoVW-2Ni (Heat XAA 3589)</u>							
Control	0	0	-57	-25	-32		17
300	1.2-1.5	1.1-1.6	98	120	109	141	15
400	2.2-2.4	3.1-3.5	162	-	148	180	9
<u>9Cr-1MoVNb</u>							
Control	0	0	-49	-37	-29		25
300	1.1-1.9	0.3-0.6	41	43	45	74	26
400	2.1-2.3	0.7-0.8	12	19	27	56	28

Selected fractured surfaces were examined by scanning electron microscopy (SEM). Fracture surfaces of the irradiated 9Cr-1MoVNb and 12Cr-1MoVW steels appeared similar to those of the steels in the unirradiated condition: ductile shear on the upper shelf and cleavage or quasi-cleavage on the lower shelf, with a combination of these in the transition region. Most observations on 12Cr-1MoVW-2Ni were similar to the steels without nickel additions. However, as seen in Fig. 1, isolated areas of a 12Cr-1MoVW-2Ni specimen irradiated at 400°C and tested in the transition region showed indications of intergranular separation.

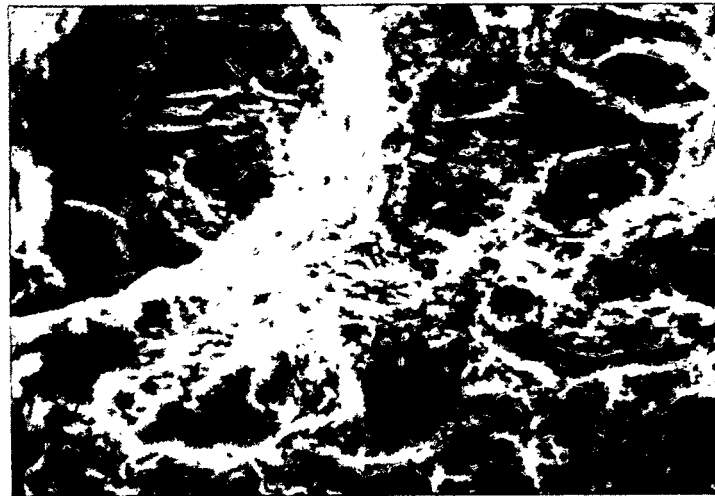


Fig. 1. Scanning electron micrograph of fracture surface of 12Cr-1MoVW-2Ni steel Charpy specimen irradiated at 400°C that shows indications of intergranular fracture.

### Discussion

The observations will first be compared with previous results, followed by a discussion of possible mechanisms to explain these and other observations.

### Comparison With Previous Work

Hu and Gelles [6] irradiated 9Cr-1MoVNb and 12Cr-1MoVW steels to 13 and 26 dpa at 390°C in the Experimental Breeder Reactor (EBR-II), a fast reactor where little helium forms. The  $\Delta$ DBTT saturated with fluence after 13 dpa at values of 54 and 124-144°C, respectively [6]. Irradiation of the 12Cr-1MoVW

heat (XAA 3787) used in this experiment had a  $\Delta$ DBTT of 122°C when irradiated to 12 dpa at 390°C in EBR-II [4]. Other studies of 12Cr-1MoVW steel irradiated in EBR-II and the Fast Flux Test Facility (FFTF) at 390-420°C indicated that saturation occurred by 10 dpa [4,19,20].

Even for the low fluences of this experiment, embrittlement, as evidenced by the shift in DBTT, was observed at both 300 and 400°C. Examination of the  $\Delta$ DBTT data in Table 2 after irradiation in HFIR at 400°C indicates that the  $\Delta$ DBTT for the 9Cr-1MoVNb (56°C) and 12Cr-1MoVW (146°C) steels approached the saturation values in a fast reactor (54 and 124-144°C, respectively) [6]. Saturation in a fast reactor occurred by 10 dpa, the lowest fluences used [4,6,19,20]. Because little helium formed in 9Cr-1MoVNb (<1 appm He) and 12Cr-1MoVW (<1.5 appm He) specimens irradiated to 2.2-2.5 dpa at 400°C in HFIR in the present tests and the  $\Delta$ DBTT of the steels approached those for irradiation in a fast reactor at 400°C, it is concluded that the saturation  $\Delta$ DBTT due to displacement damage (in the absence of a helium effect) must be reached in as little as 2 dpa.

The results for 9Cr-1MoVNb and 12Cr-1MoVW steels (Table 2) show that the  $\Delta$ DBTT was larger at 300°C than at 400°C, even though the fluence at 300°C was slightly less than at 400°C. Such a decrease in  $\Delta$ DBTT with an increase in temperature agrees with results from fast reactor irradiations at 365 to 550°C [2,4,6,19]. Fast reactor irradiation temperatures below  $\approx$ 365°C cannot be achieved, so it is not known if the 300°C values in Table 2 are saturation values.

Although the  $\Delta$ DBTT for 9Cr-1MoVNb (56°C) and 12Cr-1MoVW (146°C) after irradiation to 2.2-2.5 dpa at 400°C are similar to saturation values observed in fast reactors (54 and 124-144°C for 9Cr-1MoVNb and 12Cr-1MoVW, respectively), they are less than after 40 dpa in HFIR (202 and 242°C, respectively). The larger  $\Delta$ DBTTs after 40 dpa were attributed to the simultaneous production of helium and displacement damage in HFIR, compared to just displacement damage in a fast reactor [3,15]. Because of the small amounts of helium in the 9Cr-1MoVNb and 12Cr-1MoVW steels in the present experiment (1-1.3 appm), it is not unexpected that the steels behave as they do in a fast reactor. In both cases, helium levels were too small to affect the  $\Delta$ DBTT.

A similarity in saturation behavior between a fast-spectrum and a mixed-spectrum reactor was also observed for 1/3-size Charpy specimens of 12Cr-1MoVW irradiated in EBR-II [6] and in the mixed-spectrum Oak Ridge Research Reactor (ORR) [19]. Because of the low thermal flux in the ORR, irradiation of 12Cr-1MoVW steel to  $\approx$ 7 dpa at 330 and 400°C produced <3 appm He. The  $\Delta$ DBTT results for 7 dpa at 400°C were similar to those after irradiation to 13 and 26 dpa in EBR-II at 390°C, where similar small amounts of helium were generated [6]. Interpolation of the ORR results at 330 and 400°C to 365°C indicated good agreement between 12Cr-1MoVW irradiated to 7 dpa in ORR and irradiated to saturation (10 dpa) at 365°C in FFTF [19]. The  $\Delta$ DBTT at 330°C exceeded that at 400°C, similar to observations on temperature effects in EBR-II and the present experiment.

The 12Cr-1MoVW-2Ni steel behaved differently from the 9Cr-1MoVNb and 12Cr-1MoVW steels (Table 2) in that the  $\Delta$ DBTT for 12Cr-1MoVW-2Ni at 400°C exceeded that at 300°C and was greater than that for 12Cr-1MoVW at 300 and 400°C. Furthermore, the  $\Delta$ DBTT at 400°C was double the shift observed for 12Cr-1MoVW-2Ni irradiated in EBR-II to 12 dpa at 390°C [4]. Qualitatively, these observations on 12Cr-1MoVW-2Ni agree with those in the high-fluence HFIR irradiations [15], except that the shifts were not as great as for the previous tests. Also, in the higher fluence experiments in HFIR [15], the  $\Delta$ DBTT values at 400°C for 9Cr-1MoVNb and 12Cr-1MoVW steels were larger than those at 300°C [15], just as they were for 12Cr-1MoVW-2Ni in the present experiments and for 12Cr-1MoVW in an earlier high-fluence experiment [3].

In previous HFIR irradiations [3,7,15], higher fluences were used, which produced higher helium concentrations, even without nickel additions. The "reverse temperature effect" (i.e., a higher  $\Delta$ DBTT at 400 than 300°C) was observed for 9Cr-1MoVNb, 9Cr-1MoVNb-2Ni, 12Cr-1MoVW, and 12Cr-1MoVW-2Ni after high-fluence HFIR irradiations [3,15], but not after fast reactor irradiations [4,7]. Also, after HFIR irradiation, a larger  $\Delta$ DBTT was observed for the 9Cr-1MoVNb-2Ni and 12Cr-1MoVW-2Ni steels than for these steels without nickel. These observations were attributed to helium and indicated that as little as 30 appm helium significantly affected embrittlement at 400°C [3,15].

The most helium in the present tests formed in the 12Cr-1MoVW-2Ni irradiated at 400°C. Intuitively, this small amount of helium (3-3.5 appm) would not be expected to affect the impact toughness; however, the observations are consistent with the previous high-helium results [3,15].

Since a larger  $\Delta$ DBTT than the saturation for fast reactors and a reverse temperature effect were observed in previous HFIR experiments for both nickel-doped and undoped steels [3,15], the effects are not related to the nickel additions made to the standard compositions. In one experiment [3], 12Cr-1MoVW steel irradiated in HFIR at 400°C to  $\approx 7$  dpa and  $\approx 18$  appm He developed a  $\Delta$ DBTT of 195°C, compared to the saturation value of 124-144°C after 13 dpa in EBR-II at 390°C. After irradiation of 12Cr-1MoVW in HFIR at 400°C to  $\approx 40$  dpa and  $\approx 100$  appm He, a still larger  $\Delta$ DBTT of 242°C was observed. The 9Cr-1MoVNb irradiated to  $\approx 40$  dpa and 32 appm He at 400°C had a  $\Delta$ DBTT of 204°C, compared to a saturation at 13 dpa in EBR-II at 390°C of 56°C. All experiments contained specimens at 300°C, and a reverse temperature effect occurred in each case.

Graphical comparison of the  $\Delta$ DBTTs from HFIR and EBR-II for 9Cr-1MoVNb (Fig. 2) and 12Cr-1MoVW (Fig. 3) indicates the dichotomy of the irradiation effects in the two reactors. Figures 2 and 3 contain data from all HFIR experiments [3,5,7,15], including those at 50°C [5,7]. Data are labeled with dpa and helium concentration (in appm). The only EBR-II data shown are those of Hu and Gelles [6], because these are the only data from a single heat of steel over a range of temperatures. Fast reactor data for other heats of steel irradiated around 400°C agree with the trends in the figures [1,4].

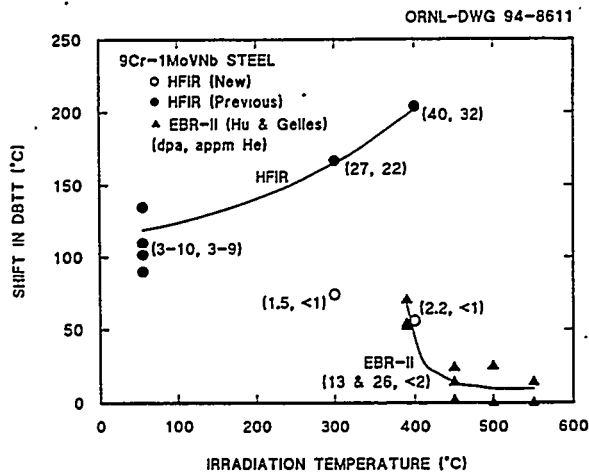


Fig. 2. A plot of the shift in DBTT against irradiation temperature for 9Cr-1MoVNb steel irradiated in HFIR and EBR-II. Numbers in parentheses adjacent to the data show the displacement damage in dpa and helium concentration in appm.

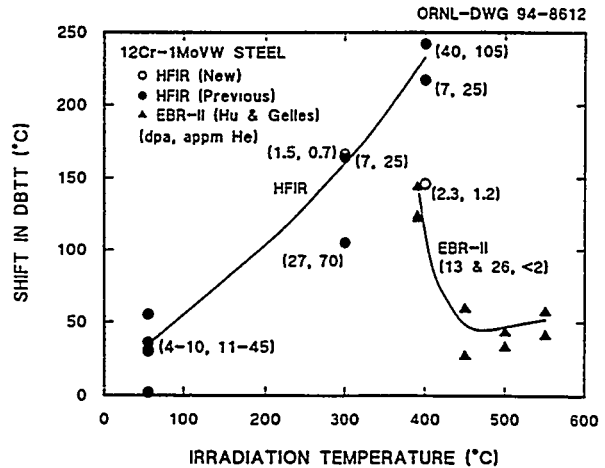


Fig. 3. A plot of the shift in DBTT against irradiation temperature for 12Cr-1MoVW steel irradiated in HFIR and EBR-II. Numbers in parentheses adjacent to the data show the displacement damage in dpa and helium concentration in appm.

The 300 and 400°C data from the present study are comparable to the fast-reactor data; therefore, these data were not used to draw the trend curves for the HFIR data. For 9Cr-1MoVNb, the  $\Delta$ DBTT for the 300°C irradiation from the present experiment falls significantly below data from HFIR after 27 dpa (Fig. 2). However, the  $\Delta$ DBTT for 12Cr-1MoVW irradiated at 300°C agrees with one point (7 dpa) from a previous HFIR experiment [3], but not with the other (27 dpa) [15], which had a much smaller  $\Delta$ DBTT. No explanation for this discrepancy for the 27 dpa irradiation exists, other than the high degree of scatter in the five specimens available for the 27 dpa tests [15] and less scatter for the eight specimens for the 7 dpa test [3].

#### Proposed Mechanism for Helium-Affected Fracture

Transmutation helium can affect the behavior of an irradiated alloy in three ways [21,22]. First, helium stabilizes vacancy clusters, which, in turn, cause an increase in the number of interstitial clusters (i.e., helium ties up vacancies and reduces interstitial-vacancy recombination). Interstitial clusters can then grow into dislocation loops and increase the strength [21,22]. Secondly, helium stabilizes the clusters to a higher temperature than in the absence of helium [21,22]. The third effect involves the migration of helium to grain boundaries during irradiation, which can then affect mechanical properties [21,22].

One clue to how helium affected fracture in the present experiments through the third helium effect is the observation that the 12Cr-1MoVW-2Ni steel irradiated to 2.2-2.4 dpa at 400°C showed indications of intergranular fracture that were not observed on the 9Cr-1MoVNb and 12Cr-1MoVW steels (Fig. 1). Previous observations on the 9Cr-1MoVNb, 9Cr-1MoVNb-2Ni, 12Cr-1MoVW, and 12Cr-1MoVW-2Ni steels irradiated to higher fluences in HFIR also showed indications of intergranular fracture [15]. Intergranular fracture was not observed after irradiation in fast reactors or in the unirradiated condition [2,6,15].

Figure 4 is a schematic diagram from Hawthorne [23] illustrating how the increase in flow stress due to irradiation hardening can cause a shift in DBTT. Hardening can be caused by radiation-produced point defects, which collect into dislocation loops to form barriers to dislocation motion, and by irradiation-induced precipitates. These two effects contribute to the hardening of steels irradiated in HFIR or a fast reactor, such as EBR-II.

Tensile studies on the nickel-doped and undoped steels irradiated in HFIR indicated that helium provided an increment of hardening above that due to radiation-produced defects and precipitates [14]. This hardening by helium, presumably through the first and second mechanisms discussed above, was concluded to saturate at around 80 appm He [14]. However, a recent reanalysis of all 400°C data [13,14] suggests that data scatter makes a definite conclusion concerning saturation at 80 appm He somewhat uncertain. What can be stated is that there is probably a slight increment of hardening at 400°C due to helium, presumably caused by the first two mechanisms discussed above. Low-temperature data indicate that the magnitude of the hardening due to helium is larger at 50°C than at 400°C [12]. Therefore, hardening by dislocation loops, precipitates, and helium could all contribute to the increase in flow stress for HFIR irradiation (Fig. 4).

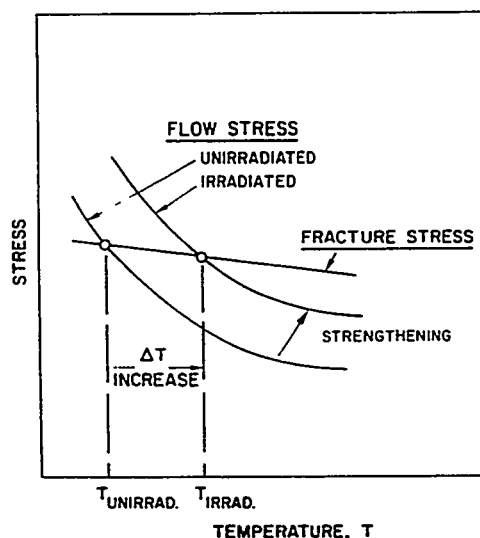


Fig. 4. Schematic diagram of mechanism by which strength increase due to irradiation causes an upward shift in the ductile-brittle transition temperature

The  $\Delta$ DBTT after HFIR irradiation at 400°C exceeded the saturation value after fast reactor irradiation and did not appear to saturate with helium concentration [15]. Thus, this shift was not caused by the increase in flow stress alone (illustrated in Fig. 4). Rather, the larger shift in the presence of helium was attributed to a lower fracture stress caused by a change in fracture mode [15,24].

An increase in DBTT can be caused by: (1) more or larger flaws, (2) less resistance to the initiation of a flaw, and (3) less resistance to the propagation of a flaw. Inclusions or carbides are likely sources of microcracks that initiate fracture in steels [25,26]. The larger  $\Delta$ DBTT for 12Cr-1MoVW than 9Cr-1MoVNb in FFTF (little helium) was attributed to the larger amounts of large precipitate particles in 12Cr-1MoVW steel [20]. The 12Cr-1MoVW contains twice as much precipitate as 9Cr-1MoVNb because it contains twice as much carbon [27].

It is now proposed that when the steels contain sufficient helium, the microcrack source could be a helium-containing bubble or bubbles on a prior-austenite grain boundary or a lath boundary. Helium is envisioned to collect into small cavities that under stress become nuclei for fracture and/or enhance crack propagation, explaining why fracture surfaces of HFIR-irradiated, helium-containing steels contain intergranular facets.

This hypothesis can be used to explain the reverse temperature effect. Formation of helium bubbles at grain boundaries will require helium diffusion to prior-austenite grain boundaries or lath boundaries. More rapid diffusion at 400°C than at 300°C means that at 400°C more helium reaches boundaries to produce larger bubbles and a larger  $\Delta$ DBTT. At 300°C, helium takes longer to reach the boundary and bubbles take longer to form. Until enough helium is available at the boundary, helium will not affect fracture.

As helium generation at 300°C is increased by higher fluences (longer diffusion times) or higher helium generation rates, the larger helium concentration will produce larger bubbles with an increase in the  $\Delta$ DBTT. This was observed for the 9Cr-1MoVNb-2Ni and 12Cr-1MoVW-2Ni irradiated to 27 dpa at 300°C, where these steels developed a larger  $\Delta$ DBTT than the steels without any nickel additions [15]. The hypothesis also explains why the  $\Delta$ DBTT for 9Cr-1MoVNb after 27 dpa in HFIR at 300°C was much larger than after 1-2 dpa at 300°C (Fig. 2), but was not as large as after the 400°C irradiation. A possible problem with this explanation is that the  $\Delta$ DBTT for 12Cr-1MoVW after 7 dpa [3] at 300°C is similar to that expected without helium in EBR-II (determined by extrapolation from 400°C) and after 1-2 dpa in HFIR (the abnormally low 27 dpa point in HFIR was ignored for this discussion). This could be explained by the  $\Delta$ DBTT in this case being determined by the larger amount of precipitate formed in 12Cr-1MoVW [20,27]. That is, even in the presence of helium, the fracture process at 300°C in 12Cr-1MoVW is controlled by the precipitates, just as it is in the absence of helium. This will be discussed further below.

### Fracture Behavior

From the above discussion, it follows that the fracture mechanism will depend on various factors, including chemical composition, irradiation temperature, and helium concentration. A comparison of Figs. 2 and 3 indicates that the  $\Delta$ DBTT for 12Cr-1MoVW irradiated in HFIR at 50°C is less than half that for 9Cr-1MoVNb [7]. The opposite is true after EBR-II irradiation at 390°C [6], where the  $\Delta$ DBTT for 12Cr-1MoVW is over twice that for 9Cr-1MoVNb. On the other hand, for irradiation in HFIR at 300 and 400°C to a high dpa, the  $\Delta$ DBTT of 12Cr-1MoVW is just slightly greater than that for 9Cr-1MoVNb.

It was previously suggested that the observations for HFIR irradiation at 50 and 300-400°C mean 9Cr-1MoVNb is more susceptible to helium [7]. As pointed out above, the results for HFIR irradiation at 300°C may mean that helium has relatively less effect on 12Cr-1MoVW because its properties are already adversely affected by the greater amount of precipitate in its microstructure. The helium effect at 300 and 400°C was assumed to cause helium-assisted intergranular fracture. At 50°C, helium diffusion will not be sufficient to affect fracture. Furthermore, 9Cr-1MoVNb (0.1% Ni) contains less helium after irradiation than 12Cr-1MoVW (0.4% Ni) [7,13]. Finally, SEM showed no change in fracture mode after irradiation at 50°C [31]. Thus, helium cannot explain why 9Cr-1MoVNb has a higher  $\Delta$ DBTT than 12Cr-1MoVW after irradiation at 50°C in HFIR [7], but has a lower  $\Delta$ DBTT after irradiation in EBR-II at 390°C.

The most logical explanation is that the change in irradiation temperature caused a change in fracture behavior for one of the steels. Support for this is found in work by Gelles et al. [28], who observed  $\delta$ -ferrite stringers on the cleavage fracture surface of 12Cr-1MoVW steel irradiated in EBR-II at 390°C [2], but not at 50°C in HFIR [28]. They concluded that the large  $\Delta$ DBTT for 12Cr-1MoVW at 390°C was due to "precipitation at  $\delta$ -ferrite stringers" in the 12Cr-1MoVW [2]. However, Gelles et al. [28] concluded that the reason for the difference between 9Cr-1MoVNb and 12Cr-1MoVW at 50°C was due to an irradiation effect on the 9Cr-1MoVNb. Carbide crystal structure alteration due to recoil dissolution was suggested as a possibility. It is now suggested that neutron irradiation at 50°C has an inherently greater relative hardening effect on 9Cr-1MoVNb than 12Cr-1MoVW, and then the magnitude of the effect reverses at higher temperatures because of the change in fracture mode of the 12Cr-1MoVW caused by precipitation.

Because of the irradiation-enhanced diffusion at 390°C in EBR-II, precipitates can form at  $\delta$ -ferrite/martensite interfaces of the 12Cr-1MoVW steel during irradiation, and these precipitates cause a change in fracture behavior. No such diffusion-assisted precipitates would be expected to form after <10 dpa at 50°C. Thus, although the  $\Delta$ DBTT of 12Cr-1MoVW at 50°C is about half as large as the  $\Delta$ DBTT of 9Cr-1MoVNb, the change in fracture process for the 12Cr-1MoVW makes the  $\Delta$ DBTT greater at the higher temperatures.

This explanation for the different relative behavior of 9Cr-1MoVNb and 12Cr-1MoVW at 50 and 390°C is supported by Anderko et al. [29], who showed that the  $\delta$ -ferrite in 12Cr steels did not by itself cause early cleavage, as suggested by other investigators. Rather, they concluded that fracture was initiated at precipitates (carbides) on the  $\delta$ -ferrite/martensite interface [2]. Therefore, the fact that  $\delta$ -ferrite stringers were not observed by Hu and Gelles on the 12Cr-1MoVW fracture surface after the 50°C irradiation [28] suggests that the absence of interface precipitation at 50°C was probably responsible for the inherently better behavior of 12Cr-1MoVW than 9Cr-1MoVNb at 50°C. At higher temperatures where precipitation occurs, the carbides on the  $\delta$ -ferrite/martensite interface cause a larger  $\Delta$ DBTT for 12Cr-1MoVW than 9Cr-1MoVNb in the absence of helium because 9Cr-1MoVNb does not contain  $\delta$ -ferrite and does not show a change in the fracture behavior with increasing temperature. This explanation implies that when helium is present, it does not necessarily have a greater effect on 9Cr-1MoVNb than 12Cr-1MoVW. Rather, the negative effect of precipitates in causing a large  $\Delta$ DBTT for 12Cr-1MoVW in the absence of helium means there will be a relatively smaller effect of helium on this steel.

It should be pointed out that no  $\delta$ -ferrite was detected in the heat of 12Cr-1MoVW (XAA 3587) used in this and other experiments [10,11], compared to a few percent found by Hu and Gelles [2]. This may mean that there was a very small amount present, but not detected, or that the more extensive radiation-induced precipitation in 12Cr-1MoVW (and not 9Cr-1MoVNb) in the temperature range 300-500°C [11,33] is responsible for the relative change in fracture behavior of 9Cr-1MoVNb and 12Cr-1MoVW between 50 and 400°C.

Figure 5 is a reproduction of the  $\Delta$ DBTT-temperature relationship of Fig. 2 for the 9Cr-1MoVNb steel with a schematic representation of how the various irradiation effects are postulated to affect fracture behavior between 50 and 400°C. Although no data are available for irradiation in fast reactors below  $\approx$ 365°C, a postulated curve for EBR-II irradiation down to 50°C has been added to the figure. Irradiation-produced defects and precipitation account for the DBTT shift in EBR-II. The relative contribution of the two processes is temperature dependent, with precipitation becoming more important with increasing temperature, but with the effect of both processes becoming negligible above  $\approx$ 450°C.

Irradiation in HFIR was postulated to lead to a further increment of hardening caused by helium [12-14,21,22], which the tensile behavior indicated also decreases to zero above 425-450°C [13]. As discussed above, the extent of hardening due to helium has not been adequately assessed, and the extent of this region is uncertain. It could be wider or narrower than indicated. In this helium-affected region and the region where hardening is dominated by defects and precipitates, the brittle region of the Charpy curve is determined by cleavage and/or quasi-cleavage.

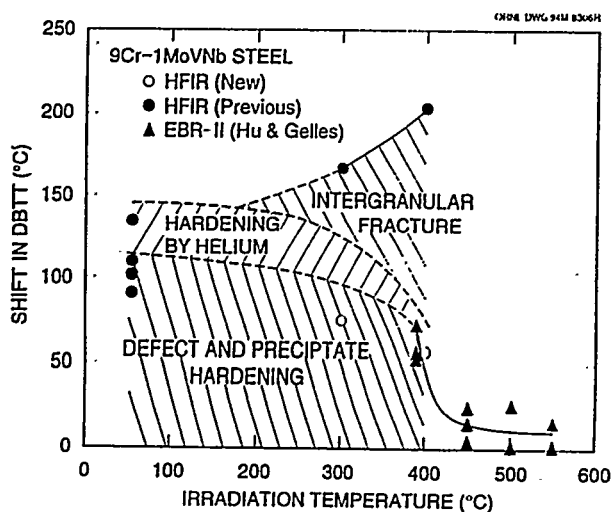


Fig. 5. The plot in Fig. 2 of the shift in DBTT against irradiation temperature for 9Cr-1MoVNb steel modified to indicate the postulated hardening and fracture mechanisms.

#### Other Considerations

Alternate explanations for the HFIR observations that do not involve helium were considered in a previous paper [15]. Those considered included the effect of other transmutation reactions with thermal neutrons in HFIR, thermal aging effects, and nickel involvement in hardening effects. None of these provided a satisfactory explanation for the observations [15].

Since the previous publication [15], a mechanism for intergranular fracture of irradiated ferritic steels was proposed by Faulkner and co-workers [30, 31]. This involves irradiation-induced segregation of impurities to prior austenite grain boundaries or lath boundaries. They demonstrated that silicon and phosphorus segregate to lath boundaries in the martensitic steel FV448 (Fe-10.7Cr-0.64Mo-0.16V-1.0Mn-0.65Ni-0.3Nb-0.38Si-0.1C) when irradiated to 46 dpa in a fast reactor at 465°C. A segregation model was developed where a linkage exists between impurities (Si, P, etc.) and irradiation-produced point defects to drive the transfer of impurities to grain boundaries [30]. Kimura et al. observed intergranular fracture in 9Cr-2Mn-1W and 12Cr-6Mn-1W steels irradiated to 10 and 25 dpa at 365°C in FFTF [32]. Based on Auger spectroscopy of fracture surfaces, they attributed the fracture behavior to radiation-induced segregation of manganese and silicon to grain boundaries. However, for segregation to explain the present observations, helium would have to enhance segregation, since no similar effect occurs when these materials are irradiated in a fast reactor.

Faulkner and co-workers also found indications of irradiation-induced segregation of nickel to lath boundaries [30] in FV448. Segregation of nickel would amplify the helium produced at a boundary in nickel-containing steels over that involving helium diffusion alone. This could enhance the effect of helium, especially on steels with 2% Ni, irradiated to both the high displacement rates of previous experiments [15] and to the low displacement rates of the present experiments. However, it should not affect the relevance of the observations for fusion, since the concentration of helium on grain boundaries in the undoped steels irradiated to high doses and in the 12Cr-1MoVW-2Ni steel irradiated to low doses should still be well below concentrations relevant for boundaries in a fusion reactor first wall.

The third region in Fig. 5 designates where intergranular fracture occurs. Around 300°C and above, the change in fracture stress that causes intergranular fracture in the presence of helium becomes important. The shape of the intergranular portion of the diagram will depend on the helium concentration, temperature, and fluence.

Similar reasoning applies for the 12Cr-1MoVW steel, although a diagram for this steel will be complicated by the increase in the  $\Delta$ DBTT with increasing temperature because of the change in fracture mode caused by precipitation. It should be noted that the 50°C tests for both steels were for relatively low-fluence irradiations (<10 dpa), and therefore, saturation may or may not have been achieved. The low-temperature irradiations also showed a slightly higher  $\Delta$ DBTT for the nickel-doped steels [7], which agrees with the hardening effect of helium observed in tensile tests of the steels irradiated at 50°C [13,14].

### Implications for a Fusion Reactor

Considerable speculation is inherent in this discussion. However, if helium plays the role postulated, then impact toughness could be affected in a fusion reactor, where large amounts of helium would be generated in the first wall. With enough helium generated during irradiation, the  $\Delta$ DBTT below 400°C could become as large or larger than at 400°C. It is unclear what might happen above 400°C, since no HFIR experiments on Ni-doped Charpy specimens have been conducted at these temperatures. The diffusion rate increases with temperature, thus increasing the rate at which helium can migrate to boundaries. On the other hand, irradiation hardening decreases rapidly above 400°C and disappears above  $\approx$ 450°C [13]. Therefore, even if helium is present on boundaries, the reduced yield stress may preclude a larger  $\Delta$ DBTT than observed for fast reactor irradiation.

It needs to be pointed out that the use of Charpy tests to evaluate embrittlement has limited applicability. A critical need exists for fracture toughness data, and an understanding of how the Charpy data are related to fracture toughness needs to be developed. Only with such data can the implications of the helium effects observed in these studies be evaluated in the context of fusion reactor design.

### SUMMARY AND CONCLUSIONS

Charpy tests were made on 9Cr-1MoVNb, 12Cr-1MoVW, and 12Cr-1MoVW-2Ni steels irradiated in HFIR at 300 and 400°C to  $\approx$ 2.5 dpa. Irradiation of the nickel-containing steels in the mixed-neutron spectrum of HFIR produced helium, but only small amounts because of the low fluence. The most helium was produced in the 12Cr-1MoVW-2Ni ( $\approx$ 3.5 appm at 400°C and 1.6 appm at 300°C). Less than 1.5 appm He was produced in the 12Cr-1MoVW and  $<$ 1 appm He in the 9Cr-1MoVNb at either 300 or 400°C.

Charpy impact behavior of the 9Cr-1MoVNb and 12Cr-1MoVW steels irradiated to the low fluences at 400°C was comparable to these steels irradiated to 13-26 dpa in a fast reactor, such as EBR-II, and was unlike the behavior after irradiation to high fluences in HFIR. That similarity between HFIR and EBR-II was attributed to the small amount of helium produced, since the difference in behavior between the steels irradiated in EBR-II and HFIR at high fluences had been previously attributed to the helium produced in HFIR. The 12Cr-1MoVW-2Ni steel after the low-fluence irradiation showed similarities with the high-fluence irradiations. An indication of intergranular fracture was observed for 12Cr-1MoVW-2Ni but not for the steels to which no nickel was added. The difference between the 9Cr-1MoVNb and 12Cr-1MoVW steels and the 12Cr-1MoVW-2Ni steel was attributed to a larger helium concentration in 12Cr-1MoVW-2Ni, even though there was only 3.5 appm He in 12Cr-1MoVW-2Ni, compared to 1 appm in the 12Cr-1MoVW.

It was postulated that when enough helium is present at 400°C (and probably 300°C), grain boundary voids can nucleate intergranular cracks that exacerbate the shift in DBTT over that in the absence of helium.

Finally, a word of caution is required. Conclusions that helium affect the impact toughness have been based on tests in different reactors and sometimes on different heats of steel. A problem with all irradiation experiments is the limited amount of reactor space available per experiment. This is especially critical for Charpy tests, where the accuracy of the curve can depend on the number of specimens tested. For some of the earlier experiments, it was necessary to generate a curve with as few as three specimens. In addition to this, the fluence each specimen receives in a capsule in HFIR depends on its position in the capsule relative to the reactor centerline. Given these conditions, it is not unreasonable to sometimes find considerable scatter in the data, as pointed out for both the tensile and Charpy data. In the near future, we intend to complete a HFIR experiment where some of these uncertainties are minimized.

## ACKNOWLEDGMENTS

Experimental work was carried out by N. H. Rouse, J. J. Henry, Jr., and E. T. Manneschildt. Dr. L. R. Greenwood of the Battelle Pacific Northwest Laboratories evaluated the flux monitors from the capsules. Helpful discussions on the work and manuscript were held with Drs. K. Farrell, J. M. Vitek, R. K. Nanstad, J. J. Kai, A. F. Rowcliffe, and E. E. Bloom.

## REFERENCES

1. F. A. Smidt, Jr., J. R. Hawthorne, and V. Provenzano, in: *Effects of Radiation on Materials: Tenth Conference, STP 725*, Eds. D. Kramer, H. R. Brager, and J. S. Perrin (American Society for Testing and Materials, Philadelphia, 1981) p. 269.
2. W. L. Hu and D. S. Gelles, in: *Ferritic Alloys for Use in Nuclear Energy Technologies*, J. W. Davis and D. J. Michel, Eds. (Metallurgical Society of AIME, Warrendale, PA, 1984) p. 631.
3. J. M. Vitek, W. R. Corwin, R. L. Klueh, and J. R. Hawthorne, *J. Nucl. Mater.* 141-143 (1986) 948.
4. W. R. Corwin, J. M. Vitek, and R. L. Klueh, *J. Nucl. Mater.* 149 (1987) 312.
5. D. S. Gelles, *J. Nucl. Mater.* 149 (1987) 192.
6. W. L. Hu and D. S. Gelles, in: *Influence of Radiation on Material Properties: 13th International Symposium (Part II)*, ASTM STP 956, F. A. Garner, C. H. Henager, Jr., and N. Igata, Eds. (American Society for Testing Materials, Philadelphia, 1987) p. 83.
7. R. L. Klueh, J. M. Vitek, W. R. Corwin, and D. J. Alexander, *J. Nucl. Mater.* 155-157 (1988) 973.
8. R. L. Klueh, J. M. Vitek, and M. L. Grossbeck, in: *Effects of Irradiation on Materials: Eleventh Conference, ASTM STP 782*, H. R. Brager and J. S. Perrin, Eds. (American Society for Testing Materials, Philadelphia, 1982) p. 648.
9. J. M. Vitek and R. L. Klueh, in: *Ferritic Alloys for use in Nuclear Energy Technologies*, J. W. Davis and D. J. Michel, Eds. (The Metallurgical Society, Warrendale, Pennsylvania, 1984) p. 551.
10. J. M. Vitek and R. L. Klueh, *J. Nucl. Mater.* 122 & 123 (1984) 254.
11. P. J. Maziasz, R. L. Klueh, and J. M. Vitek, *J. Nucl. Mater.* 141-143 (1986) 929.
12. R. L. Klueh and J. M. Vitek, *J. Nucl. Mater.* 161 (1989) 13.
13. R. L. Klueh and J. M. Vitek, *J. Nucl. Mater.* 150 (1987) 272.
14. R. L. Klueh and P. J. Maziasz, *J. Nucl. Mater.* 187 (1992) 43.
15. R. L. Klueh and D. J. Alexander, *J. Nucl. Mater.* 187 (1992) 60.
16. W. R. Corwin, R. L. Klueh, and J. M. Vitek, *J. Nucl. Mater.* 122 & 123 (1984) 343.
17. W. R. Corwin and A. M. Houglund, in: *The Use of Small-Scale Specimens for Testing Irradiated Material*, ASTM STP 888, W. R. Corwin and G. E. Lucas, Eds. (American Society for Testing and Materials, Philadelphia, 1986) p. 325.

18. D. J. Alexander, R. K. Nanstad, W. R. Corwin, and J. T. Hutton, Applications of Automation Technology to Fatigue and Fracture Testing, ASTM STP 1092, A. A. Braun, N. E. Ashbaugh, and F. M. Smith, Eds. (American Society for Testing and Materials, Philadelphia, 1990) p. 83.
19. R. L. Klueh and D. J. Alexander, in: Effects of Radiation on Materials: Fifteenth International Symposium, ASTM STP 1125, R. E. Stoller, A. S. Kumar, and D. S. Gelles, Eds. (American Society for Testing Materials, Philadelphia, 1992) p. 1256.
20. R. L. Klueh and D. J. Alexander, J. Nucl. Mater. 191-194 (1992) 896.
21. K. Farrell, Radiation Effects 53 (1980) 175.
22. K. Farrell, P. J. Maziasz, E. H. Lee, and L. K. Mansur, Radiation Effects 78 (1983) 277.
23. J. R. Hawthorne, in: Treatise on Materials Science and Technology, Vol. 25 (Academic Press, Inc., New York, 1983) p. 461.
24. G. E. Lucas and D. S. Gelles, J. Nucl. Mater. 155-157 (1988) 164.
25. R. W. Hertzberg, Deformation and Fracture Mechanics of Engineering Materials, 3rd Edition (John Wiley & Sons, New York, 1989) p. 253.
26. C. J. McMahon, Jr., Fundamental Phenomena in the Materials Sciences, Vol. 4, L. J. Bonis, J. J. Duga, and J. J. Gilman, Eds. (Plenum Press, New York, 1967) p. 247.
27. J. M. Vitek and R. L. Klueh, Met. Trans. A, 14A (1983) 1047.
28. D. S. Gelles, W. L. Hu, F. H. Huang, and G. D. Johnson, Alloy Development for Irradiation Performance, Semiannual Progress Report for Period Ending September 30, 1983, U. S. Department of Energy, Office of Fusion Energy, DOE/ER-0045/11 (March 1984) p. 115.
29. K. Anderko, L. Schafer, and E. Materna-Morris, J. Nucl. Mater. 179-181 (1991) 492.
30. R. G. Faulkner, E. A. Little, and T. S. Morgan, J. Nucl. Mater. 191-194 (1992) 858.
31. R. G. Faulkner, S. Song, and P. J. Flewitt, J. Nucl. Mater. to be published.
32. A. Kimura, L. A. Charlot, D. S. Gelles, D. R. Baer, and R. H. Jones, J. Nucl. Mater. 191-194 (1992) 885.